Light scattering effect of submicro-textured Ag/Al composite films prepared at lower substrate temperatures*

Tang Ping-Lin(唐平林)[a], Wu Yong-Gang(吴永刚)[a]†, Tong Guang-De(童广德)[b], Xia Zi-Huan(夏子奂)[a], Liu Ren-Chen(刘仁臣)[a], Liang Zhao-Ming(梁钊铭)[a], and Zhou Jian(周 建)[a]

[a] *Department of Physics, Institute of Precision Optical Engineering, Tongji University, Shanghai* 200092, *China*
[b] *National Electromagnetic Scattering Laboratory, Institute of No.* 802, *Shanghai* 200090, *China*

(Received 12 October 2012; revised manuscript received 27 February 2013)

We present a new and practical approach for preparing submicro-textured silver and aluminum (Ag/Al) double-structured layers at low substrate temperatures. The surface texturing of silver and aluminum double-structured layers was performed by increasing the deposition temperature of the Al layers to 270 °C. The highly submicro-textured silver and aluminum double-structured layers were prepared by thermal evaporation on quartz glasses and their surface microstructure, light scattering properties, and thermal stability were investigated. Results showed that the highly submicro-textured Ag/Al composite films prepared at low substrate temperatures used as back reflectors not only can enhance the light scattering and have good thermal stability, but also have good adhesion properties. In addition, their fabrication is low cost and readily carried out.

Keywords: random submicro-textured Ag/Al composite films, light scattering

PACS: 88.40.jj, 68.55.jm, 68.49.–h, 73.50.Bk **DOI:** 10.1088/1674-1056/22/7/078801

1. Introduction

Thin-film silicon solar cells have been the focus of a great number of studies due to the considerable decrease in silicon consumption in their fabrication, leading to the reduction in their manufacturing cost. Nevertheless, thin film silicon solar cells display a major disadvantage in comparison with their bulk counterpart. The complete absorption of the incident sun-light, particularly in the wavelength range from 600 nm to 1100 nm, can not be achieved due to the limited thickness of the silicon film layer, which is typically 1–4 μm. Therefore, how to trap light efficiently, which will lead to the enhancement in the short-circuit current J_{sc}, becomes the focus of this research area and has been studied extensively in recent decades. A light trapping technique utilizing a textured back reflector (BR), which can achieve a high J_{sc} without requiring a significant increase in the thickness of the Si layer, plays a critical role in improving the efficiency of thin-film silicon solar cells.[1] The absorption enhancement thus achieved is due to light scatterings and has been discussed.[2] The thin-film solar cells using a textured back reflector increase the optical path length of the incident light, because the light is scattered by the textured surface to different directions instead of specular reflection, which enhances the total internal reflection at the interfaces within the cells. Theoretically, by ideal light trapping, which can be achieved through a perfect random texture, the optical path length in a material with a refractive index of n is enhanced by a factor of $4n^2$.[3] So far, various randomly textured back reflectors/substrates have been realized using SnO_2,[4,5] ZnO,[6–11] glass,[12,13] plastic films,[11] and Ag.[14–16] In addition, a unique periodically textured back surface reflector (BSR) fabricated by using the anodic oxidation of Al has been studied.[17] From the above authors' studies, we can conclude that the efficiency of thin film silicon solar cells is improved by replacing the flat back reflectors with various optimal textured ones.

Aluminum (Al) and silver (Ag) are the most widely used materials in the back reflectors of solar cells. The former is adopted due to its low price, good adhesion properties, and ease of handling. It allows us to prepare textured surfaces at low substrate temperatures owing to its low melting point.[18,19] The major drawbacks of using Al films as back reflectors reside in their low total reflectance in the wavelength region over which solar cells operate and the occurrence of interband absorption at an undesirable wavelength ($\sim$ 800 nm).[20] The latter is adopted due to its excellent total reflectance in the desired wavelength region and good electrical conductivity. The major drawbacks of using Ag films as back reflectors reside in its high cost and the high substrate temperature required for preparing textured surfaces.[16,21] In this contribution, a new and practical approach for preparing submicro-textured silver and aluminum double-structured layers at low substrate temperatures is proposed. Submicro-textured Ag/Al composite films are fabricated on thick quartz glass substrates by thermal evaporation deposition. By controlling the substrate temperature for depositing the Al layer,

*Project supported by the National Natural Science Foundation of China (Grant No. 60977028) and the Key Project Foundation of Shanghai, China (Grant No. 09JC1413800).

†Corresponding author. E-mail: ygwu@tongji.edu.cn

© 2013 Chinese Physical Society and IOP Publishing Ltd

the changes in the surface characteristics of Ag/Al composite films are investigated systematically. Light-scattering properties, the correlation between the surface morphology of the composite films and the haze, and the thermal stability of the highly submicro-textured composite films are investigated and discussed.

2. Experiment

The Ag (99.99%) and Al (99.9%) were used as the evaporation materials. Al layers were deposited on 2-mm thick quartz glass substrates by thermal evaporation under a base pressure of 5×10^{-4} Pa. The deposition rate was 1.2 nm/s. The substrate temperature for depositing the Al layers was varied from room temperature to 270 °C to induce the changes in surface morphology. The film thickness of the Al layers was 400 nm. Next Ag layers of thickness 140 nm were deposited on the prepared Al layers at room temperature by thermal evaporation under a base pressure of 9×10^{-4} Pa. The deposition rate was 0.2 nm/s. Thus, Ag/Al composite films with different random textures were acquired. The microstructure and surface roughness of the deposited Ag/Al composite films were examined by atomic force microscopy (AFM) analysis. The total reflectance R_{total} is the sum of the specular and diffuse reflectance for a rough interface. The border angle θ_{inf} between the specular light and the diffuse light is equal to the aperture angle of the specular opening in the integrating sphere, which is used to measure the total and diffuse reflectance. In our case, $\theta_{\text{inf}} = \pi/36 = 5°$. The total reflectance using integrating sphere and the specular reflectance (R_{specular}) of the Ag/Al composite films were measured in the spectral range from 300 nm to 1100 nm by using a UV–Vis–NIR spectrophotometer (Cary 5000). The diffuse reflectance (R_{diffuse}) of the Ag/Al composite films in the spectral range from 300 nm to 1100 nm was obtained by $R_{\text{diffuse}} = R_{\text{total}} - R_{\text{specular}}$. The angular resolved scattering (ARS) intensity of the optimal composite films was measured by scattering measurement systems (Light TEC Reflect 180). The thermal stability of the prepared random submicro-textured composite films was investigated by heat treatment. The heat-treatment process is as follow. The Ag/Al composite films of which the Al layers were deposited at 270 °C were put into a vacuum chamber. When the vacuum chamber was evacuated to a base pressure of 5×10^{-4} Pa, the temperature of the sample was increased to 50 °C by iodine tungsten light radiation and kept at that temperature for 1 h. After that, the temperature of the sample was raised to 100 °C, 150 °C, 200 °C, and 220 °C and kept for 1 h at each temperature. Finally, natural cooling in the vacuum chamber was performed. The above process was carried out at a pressure below 2×10^{-3} Pa.

3. Results and discussion

3.1. Surface texture of the Ag/Al composite films

A variety of textures of the films were obtained by changing the deposition temperature of the substrate layer, as proposed in the structure zone model (SZM).[18,19,22–24] In the growth processes of pure metal (basis SZM) and multiphase or impurity containing metal films (real SZM), the structural evolutions of the films are commonly controlled by changing the parameter T_s/T_m, where T_s is the substrate temperature and T_m is the melting point of the film material. In our studies, different surface microstructures were obtained when the Al layer of the Ag/Al composite films was deposited at the substrate temperatures of room temperature, 200 °C, and 270 °C. The temperatures were chosen in the range consistent with the structure zones T and II in the SZM. The accompanying T_s/T_m values were 0.30, 0.47, and 0.55, respectively, as the melting point of Al is 993.04 K.

Figure 1 shows the changes in the surface microstructure of Ag/Al composite films induced by increasing the substrate temperature for depositing the Al layers. As shown in Fig. 1, the surface morphology of the Ag/Al composite films with the Al layer deposited at room temperature (sample (a)) is composed of columns of 200–300 nm, and the size distribution is uniform. The microstructure is a pronounced elongated columnar structure. The root-mean-square (RMS) roughness is 6 nm. When the substrate temperature for depositing the Al layer of Ag/Al composite films is increased to 200 °C (sample (b)), the sizes of the columns are increased to 500–800 nm in some partial directions, and the size distribution is no longer uniform. The heights of the columns are very unevenly distributed in the whole area. The RMS roughness obtained is 42.3 nm. When the substrate temperature for depositing the Al layer of Ag/Al composite films is increased to 270 °C (sample (c)), the surface feature becomes coarse. Columns of size 1000–1500 nm are found in the whole area. The surface microstructure is a modulated texture which consists of small pyramids on the top of larger columnar crystals. The RMS roughness obtained reaches 47.1 nm. In this case, the crystallites are nearly random or only weakly textured and the columnar structure is elongated for the film whose Al layer is deposited at the room temperature, which corresponds to the highest part of zone T ($T_s/T_m \sim 0.3$). By increasing the substrate temperature for depositing the Al layer to 200 °C, corresponding to zone II ($T_s/T_m \sim 0.4$–0.5), the surface becomes rough and the microstructure grows in some partial directions due to the pronounced orientation selection to decrease in the total grain boundary area as well as the minimization of the interface and surface energy and large grains with low surface and interface energy growth at the expense of smaller or unfavorably oriented grains. With the substrate temperature for depositing the Al layer increased up to 270 °C, corresponding

to the higher temperature region of zone II ($T_s/T_m \sim 0.5$–0.6) in which the orientation selection is completed during coalescence and secondary recrystallization, also called abnormal grain growth, followed, a state is reached where it is energetically more favorable to grow only in the lateral dimensions of the grains due to significant surface and bulk diffusion and abnormal grain growth resulting in the height of the columnar reducing.

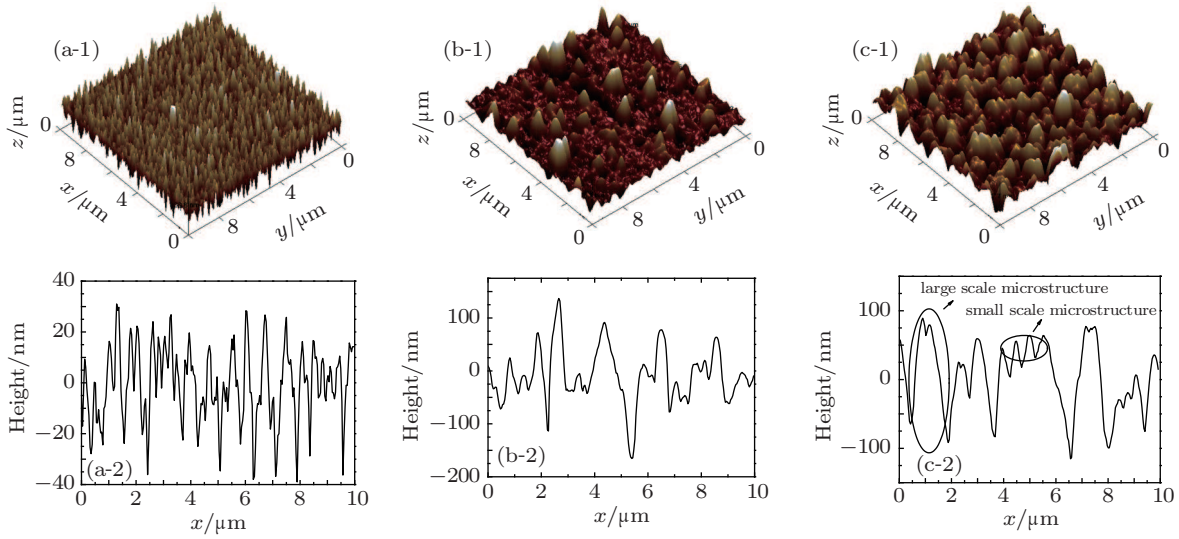


Fig. 1. (color online) Three-dimensional AFM images and cross sections along one AFM scan line on 10 μm×10 μm area of Ag/Al composite films prepared at different substrate temperatures for depositing the Al layers: (a) room temperature, (b) 200 °C, (c) 270 °C.

3.2. Haze parameters of the Ag/Al composite films

In order to investigate the light scattering properties of the Ag/Al composite films, the haze parameter $H_R = R_{diffuse}/R_{total}$ is examined, and the results are shown in Fig. 2. The absorption peak at wavelength $\sim$ 320 nm is attributed to the bulk plasmon (BP) of Ag,[20] while the absorption peak with its tail at wavelength $\sim$ 350 nm is associated with the surface plasmon (SP) of Ag.[25] The wavelength of SP shifts towards shorter ones as the refractive index n of the embedding medium increases.[26] The absorption peak and its absorption tail are quite sensitive to the surface morphology of the Ag/Al composite films. For the incident light wavelengths from 350 nm to 600 nm, the R_{total} of samples (b) and (c) are smaller than that of sample (a) due to the spread of the SP peak, which can be influenced by the surface morphology and the parasitic absorption caused by rough surface and oxidation of Ag. For the incident light wavelengths from 350 nm to 600 nm, R_{total} can be optimized by varying the deposition rate, film thickness, and the chamber pressure of Ag layer due to the adjustments of the SP absorption peak and its absorption tail.[27] Therefore, it is expected that the R_{total} of sample (c) can be improved by optimizing the deposition rate, film thickness, and the chamber pressure of Ag layer. Besides, for wavelengths from 350 nm to 600 nm, the incident light is mostly absorbed before reaching the rear surface in the solar cells. Therefore, the total and diffuse reflectances of the Ag/Al composite films for the incident light between 600 nm and 1100 nm are the focus of our study.

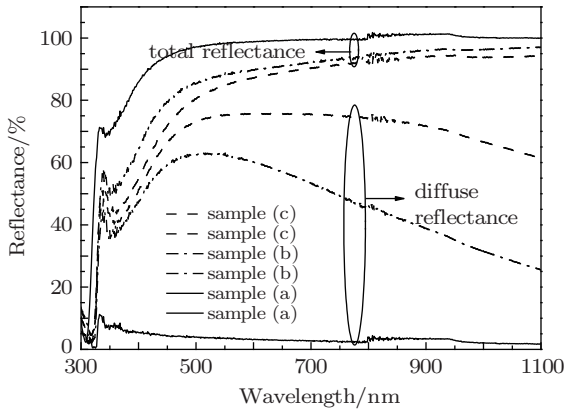


Fig. 2. Total reflectance R_{total} and diffuse reflectance $R_{diffuse}$ of the Ag/Al composite films with the Al layer deposited at room temperature (solid line), 200 °C (dash dot), and 270 °C (dash).

As shown in Fig. 2, in the wavelength range between 600 nm and 1100 nm, the average R_{total} of sample (a) is over 95%, its average $R_{diffuse}$ has not reached 5%; for sample (b), the average R_{total} is over 90%, the average $R_{diffuse}$ is only 40%; the average R_{total} of sample (c) is about 90%, and its average $R_{diffuse}$ is over 60%. For sample (c), $R_{diffuse}$ is remarkably increased as compared with that of the other samples with the Al layer prepared at lower deposition temperatures. Compared with the highly textured Ag back reflector,[16,21] which is obtained at the high deposition temperature of 500 °C and has a large film thickness above 500 nm, sample (c) possesses better

R_{diffuse} in the wavelength range between 800 nm and 1100 nm, lower deposition temperature, and less Ag consumption. For rough interfaces (the surface characteristics are defined by statistical parameters: RMS σ and correlation length l), when the RMS of the interfaces is comparable to or smaller than the effective wavelength of the medium at normal incidence and the correlation length is larger than the wavelength of light, the scale scattering theory can be applied to determine the haze factor H_{R},[4,28] and the haze factor is related to RMS σ, wavelength λ, and the refractive index of the medium of incidence (n_0) by

$$H_{\text{R}} = R_0(1 - \exp[-(4\pi\sigma n_0\lambda)^2]), \tag{1}$$

where R_0 is the total reflectance of the rough interfaces.

The H_{R} of the Ag/Al composite films with the Al films deposited at different temperatures are plotted in Fig. 3, where the total reflectance is equal to that measured and shown in Fig. 2 and n_0 is equal to 1 for the wavelength between 400 nm and 1100 nm. As shown in Fig. 3, for the wavelength between 400 nm and 600 nm, the calculated haze, which increases when the RMS values become larger, is in good agreement with that in the measurement. The calculated haze, which increases with increasing RMS roughness and decreases with increasing wavelength for the wavelength between 600 nm and 1100 nm, is also in good agreement with that in the measurement. However, noticeable quantitative disagreement between calculated and measured H_{R} is also found. Equation (1) presents a good approximation of haze parameters only if the roughness of the interface is completely random and has a normal (Gaussian) height distribution. Besides, as mentioned above, the theory requires the correlation length of the interface to be much larger than the wavelength of light to neglect shadowing and multiple-scattering effects at the rough interface. For the analyzed samples and the wavelengths studied, the disagreement may be due to that the height distribution deviates from the normal distribution, which is proposed in the film growth at the higher temperature region zone II $(T_{\text{s}}/T_{\text{m}} \sim 0.5\text{–}0.6)$,[22] and $l \gg \lambda$ is violated, which can be found and estimated from Fig. 1. For sample (c) and the wavelengths studied, the noticeable quantitative disagreement may be negatively correlated with the different geometrical features integrated in a modulated surface texture[29] which consists of small pyramids on the top of larger columnar crystals shown in Fig. 1. For the wavelength between 400 nm and 500 nm, the reason for disagreement between the calculation with Eq. (1) and the measurement of H_{R} may be that the incident light is in the region of SP's absorption tail, which is quite sensitive to the surface morphology of the Ag/Al back reflectors and the deposition rate, film thickness, and the chamber pressure of the Ag layer.

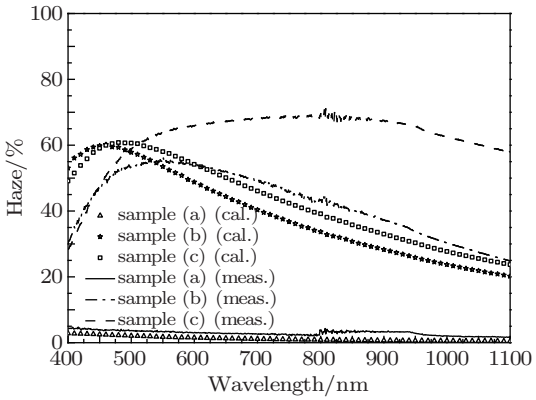


Fig. 3. Calculated and measured haze factors in the reflection of the Ag/Al composite films with different RMS values.

From the above results and discussion, it is expected that the enhanced light scattering properties of the textured surfaces of sample (c) are favorable for increasing the optical path length in thin μc-Si:H layers as well as a-Si:H layers to improve the light trapping.

3.3. Angular resolved scattering intensity distribution of the Ag/Al composite films

In Fig. 4, the angular resolved scattering (ARS) intensity distribution of the reflected light of sample (c) in the atmosphere, measured in the plane normal to the scattering interface, is shown. The direction of the outgoing radiation is described by the spherical angles θ and ϕ, where θ is the elevation angle and ϕ is the azimuthal angle of the outgoing radiation. The reflected light intensity at θ from -3° to 3° is not meaningful,[30] because the light lamp prevents the reflected light from entering into the detector for the incident light from 400 nm to 1000 nm. The solid, dashed, and dash-dot lines show angular resolved scattering intensities with $\phi_1 = 30^\circ$, $\phi_2 = 90^\circ$, and $\phi_3 = 200^\circ$, respectively. We can get the angular resolved scattering intensity distribution $D_{\text{ARS}}(\phi, \theta_0)$[31] $\approx$ constant, where θ_0 is a fixed value in the range from -90° to 90° and ϕ is a variable. This implies that, up to noise due to the limited sampling size of the interface, the angular resolved scattering intensity is independent of ϕ. In general, a thin-film solar cell consists of a front transparent conducting oxide (TCO) layer, a doped Si layer, and a rear TCO/Ag layer. The aluminum-doped zinc oxide (ZnO:Al) film is commonly used as the TCO layer between the silicon and the metallic contact as a part of the back reflector to improve the optical properties and to act as a diffusion barrier.[31] In preparing a thin film solar cell, an approximately 80-nm thick aluminum-doped zinc oxide (ZnO:Al) film is deposited on the back reflector. Thus, in this case, the critical (escaping) angle θ_{c} is defined as

$$\theta_{\text{c}} = \arcsin(n_{\text{air}}/n_{\text{Si:H}}) \approx 16^\circ. \tag{2}$$

Such a thin layer does not affect the total internal reflection. For the back reflector, the total scattering intensity of the total internal reflection at the interface within the cells is obtained

by integrating[30,32] (without writing explicitly the dependence on the wavelength)

$$I_c = \int D_{ARS}(\phi, \theta) \, d\Omega. \quad (3)$$

For random textures and the perpendicular incidence, the angular resolved scattering intensity is independent of ϕ. Therefore $D_{ARS}(\phi, \theta)$ can be simplified to $D_{ARS}(\theta)$ by integrating out the azimuthal angle ϕ. The ARS is obtained from Fig. 3, so we can get the expression of the total scattering intensity for elevation angles θ between θ_1 and θ_2

$$I_c = \int_0^{2\pi} d\phi \int_{\theta_1}^{\theta_2} D_{ARS}(\theta) \sin\theta \, d\theta. \quad (4)$$

Therefore the scattering intensity of the total internal reflection at the interface within the cells is

$$I_c = \int_0^{2\pi} d\phi \int_{4\pi/45}^{\pi/2} D_{ARS}(\theta) \sin\theta \, d\theta. \quad (5)$$

From Ref. [33], we find that the angular resolved scattering intensity distribution of ZnO:Al–Ag/Al interface is independent of ϕ and θ and equals N times that of the air-Ag/Al interface, so the calculation indicates

$$I_c / I \approx 55\%,$$

where I is the total intensity of the outgoing radiation. Meanwhile, we find in Fig. 2 that the intensity of the specular reflectance is about 30% of the incident light from 400 nm to 1000 nm.

In Subsection 3.2, the $R_{diffuse}$ of sample (c) is about 70% for the incident light from 600 nm to 1100 nm in the air. The scattering intensity of the total internal reflection at the interface within the cells in the large angle region ($15^\circ < \theta < 90^\circ$) is about 55%, and the scattering intensity is about 34% in the larger angle region ($30^\circ < \theta < 90^\circ$) for the incident light from 400 nm to 1000 nm. Therefore, it is expected that the Ag/Al composite films with the Al layer deposited at 270 °C as a back reflector in thin-film silicon solar cells can enhance the light trapping and improve the efficiency of the thin-film silicon solar cells.

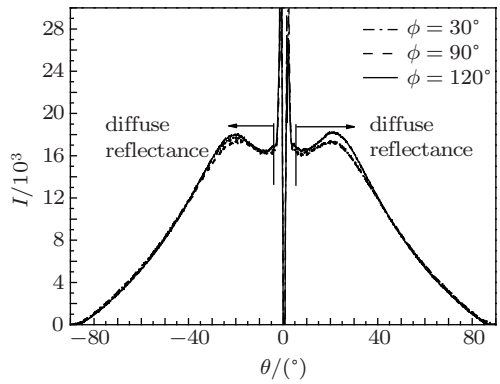


Fig. 4. Angular resolved scattering intensity distribution of the Ag/Al composite films with the Al layer prepared at 270 °C, the solid, dashed, and dash-dot lines show angular resolved scattering intensities of different directions.

3.4. Thermal stability of the Ag/Al composite films

Generally, the TCO and the Si absorption layers are fabricated on the back reflectors at a certain temperature (200–250 °C)[16,17] to improve the efficiency of solar cells. Therefore, the thermal stability of sample (c) should be investigated through annealing at different temperatures in vacuum. The surface microstructure and the scattering properties of sample (c) after heat treatment are shown in Fig. 5. The surface microstructure and the scattering properties of sample (c) after heat treatment are similar to those before treatment. The RMS of sample (c) after heat treatment increases slightly, and the absorption peak which is caused by the SP of Ag has a slight blue-shift. The reason for the results may be that the temperature of heat treatment is too low, so the atoms of the Al film do not have enough energy to break the texture with which the Ag/Al composite films have a minimized overall surface and interface energy and the Ag film has a good thermal stability below 300 °C. From above, sample (c) has a good thermal stability, which is very useful for fabricating film solar cells.

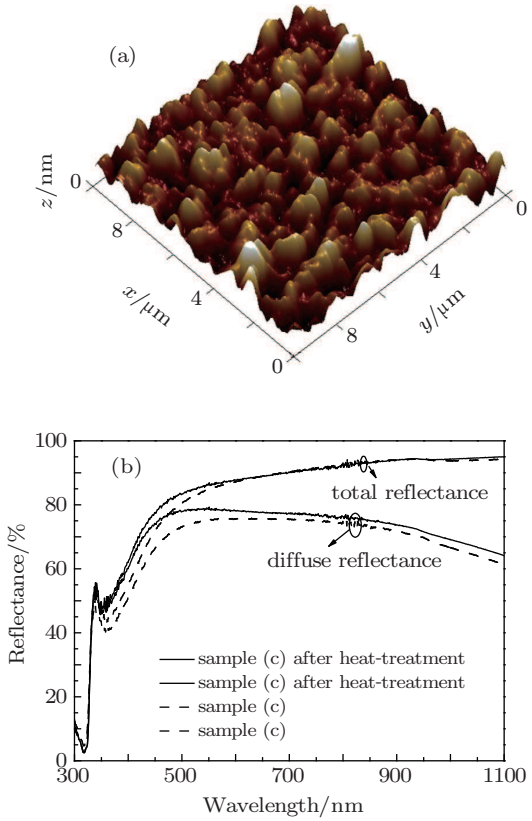


Fig. 5. (color online) (a) AFM image and (b) the total and diffuse reflectance of sample (c) after heat treatment.

4. Conclusions

In this work, thermal evaporated Ag/Al composite films with highly submicro-textured surfaces were successfully prepared on 2-mm thick quartz glass substrates by changing the

substrate temperature for depositing the Al layers. The surface microstructure, light scattering properties, and thermal stability of the submicro-textured composite films fabricated at low substrate temperatures were investigated. By increasing the substrate temperature for depositing the Al layers, the surface of the Ag/Al composite films was texturized, resulting in the increase of the diffuse reflectance of the Ag/Al composite films for the wavelength between 600 nm and 1100 nm. Using sample (c) as the back reflector, the scattering intensity of total internal reflection at the interface within the cells was about 55% for the incident light with wavelengths from 400 nm to 1000 nm and the diffuse reflectance was about 70% for the incident light with wavelengths from 600 nm to 1100 nm. The prepared submicro-textured Ag/Al composite films possessed the following properties: (i) low cost of preparation, easy preparation; (ii) better adhesion properties compared with the pure Ag random texture back reflector; (iii) lower desposition temperatures (below 270 °C) at which the highly textured surface was obtained due to the low melting point of Al compared with the highly textured Ag back reflector,[16] which was desiposed at 500 °C; (iv) perfect scattering properties in the wavelength range where the solar cells are operating; (v) good thermal stability.

References

[1] Yang J, Yan B, Yue G and Guha S 2009 *MRS Symposia Proceedings* 2009 *Pittsburgh*, USA No. 1153

[2] Poruba A, Fejfar A, Remeš Z, Špringer J, Vaněček M and Kočka J 2000 *J. Appl. Phys.* **88** 148

[3] Yablonovitch E 1982 *J. Opt. Soc. Am.* **72** 899

[4] Krč J, Zeman M, Smole F and Topič M 2002 *J. Appl. Phys.* **92** 749

[5] Matsui T, Tsukiji M, Saika H, Toyama T and Okamoto H 2002 *J. Non-Cryst. Solids* **299–302** 1152

[6] Berginski M, Hüpkes J, Schulte M, Schöpe G, Steibig H, Rech B and Wuttig M 2007 *J. Appl. Phys.* **101** 074903

[7] Rech B, Kulth O, Repmann T, Roschek T, Springer J, Müller J, Finger F, Steibig H and Wagner H 2002 *Sol. Energy Mater. Sol. Cells* **74** 439

[8] Nasuno Y, Kohama N, Nishimura K, Hayakawa T, Taniguchi H and Shimizu M 2006 *Appl. Phys. Lett.* **88** 071909

[9] Söderström T, Huag F J, Terrazzoni-Daudrix V and Ballif C 2008 *J. Appl. Phys.* **103** 114509

[10] Fäy S, Kroll U, Bucher C, Vallat-Sauvian E and Shah A 2005 *Sol. Energy Mater. Sol. Cells* **86** 385

[11] Terrazzoni Daudrix V, Guillet J, Freitas F, Shah A, Ballif C, Winkler P, Ferreloc M, Benagli S, Niquille X, Fischer D and Morf R 2006 *Prog. Photovoltaics* **14** 485

[12] Deckman H W, Wronski C R and Witzke H 1983 *J. Vac. Sci. Technol. A* **1** 578

[13] Niira K, Senta H, Hakuma H, Komoda M, Okui H, Fukui K, Arimune H and Shirasawa K 2002 *Sol. Energy Mater. Sol. Cells* **74** 247

[14] Takano A, Uno M, Tanda M, Iwasaki S, Tanaka H, Yasuda J and Kamoshita T 2004 *Jpn. J. Appl. Phys.* **43** L277

[15] Franken R H, Stolk R L, Li H, Van der Werf C H, Rath J K and Schropp R E I 2007 *J. Appl. Phys.* **102** 014503

[16] Cho J S, Baek S and Yoon K H 2007 *Curr. Appl. Phys.* **11** S2

[17] Sai H, Fujiwara H, Kondo M and Kanamori Y 2008 *Appl. Phys. Lett.* **93** 143501

[18] Petrov I, Barna P B, Hultman L and Greene J E 2003 *J. Vac. Sci. Technol. A* **21** s117

[19] Adamik M, Barna P B and Tomov I 1998 *Thin Solid Films* **317** 64

[20] Jäger K, Fischer M, Van Swaaij R A C M M and Zeman M 2012 *J. Appl. Phys.* **111** 083108

[21] Cho J S, Baek S, Park S H, Park J H, Jinsu Y and Yoon K H 2012 *Sol. Energy Mater. Sol. Cells* **102** 50

[22] Thorton J A 1977 *Annu. Rev. Mater. Sci.* **7** 239

[23] Messier R, Griri A P and Roy A R 1983 *T. Vac. Sci. Technol. A* **2** 500

[24] Xu M C, Qian H J, Liu F Q, Krash I, Lai W Y and Wu S C 2000 *Chin. Phys. Lett.* **17** 595

[25] Plummer W, Tsuei K D and Kim B O 1995 *Phys. Res. B.* **96** 448

[26] Liebsch A 1993 *Phys. Rev. Lett.* **71** 145

[27] Springer J, Poruba A, Müllerova L, Vanecek M, Kluth O and Rech B 2004 *J. Appl. Phys.* **95** 1427

[28] Krč J, Zeman M, Smole F and Topic M 2003 *Thin Solid Films* **426** 296

[29] Isabella O, Krč J and Zeman M 2010 *Appl. Phys. Lett.* **97** 101106

[30] Domine D, Haug F J, Battaglia C and Ballif 2010 *J. Appl. Phys.* **107** 044504

[31] Gupta R, Dyer M J and Weimer W A 2002 *J. Appl. Phys.* **92** 5264

[32] Sven S, Angela D, Luisa C, Andreas T, Penalver D H and Harvey J E 2011 *Opt. Express* **19** 9820

[33] Müller J, Rech B, Springer J and Vanecek M 2004 *Sol. Energy* **77** 917